GEOLOGY | THE GEOLOGICAL SOCIETY OF AMERICA®

https://doi.org/10.1130/G49153.1

Manuscript received 4 February 2021
Revised manuscript received 5 July 2021
Manuscript accepted 7 July 2021

River sinuosity describes a continuum between randomness and ordered growth

Ajay B. Limaye[1], Eli D. Lazarus[2], Yuan Li[1] and Jon Schwenk[3]
[1]Department of Environmental Sciences, University of Virginia, Charlottesville, Virginia 22904, USA
[2]Environmental Dynamics Lab, School of Geography and Environmental Science, University of Southampton, Highfield, Southampton SO17 1BJ, UK
[3]Earth and Environmental Science Division, Los Alamos National Laboratory, Los Alamos, New Mexico 87545, USA

ABSTRACT

River channels are among the most common landscape features on Earth. An essential characteristic of channels is sinuosity: their tendency to take a circuitous path, which is quantified as along-stream length divided by straight-line length. River sinuosity is interpreted as a characteristic that either forms randomly at channel inception or develops over time as meander bends migrate. Studies tend to assume the latter and thus have used river sinuosity as a proxy for both modern and ancient environmental factors including climate, tectonics, vegetation, and geologic structure. But no quantitative criterion for planform expression has distinguished between random, initial sinuosity and that developed by ordered growth through channel migration. This ambiguity calls into question the utility of river sinuosity for understanding Earth's history. We propose a quantitative framework to reconcile these competing explanations for river sinuosity. Using a coupled analysis of modeled and natural channels, we show that while a majority of observed sinuosity is consistent with randomness and limited channel migration, rivers with sinuosity ≥1.5 likely formed their geometry through sustained, ordered growth due to channel migration. This criterion frames a null hypothesis for river sinuosity that can be applied to evaluate the significance of environmental interpretations in landscapes shaped by rivers. The quantitative link between sinuosity and channel migration further informs strategies for preservation and restoration of riparian habitat and guides predictions of fluvial deposits in the rock record and in remotely sensed environments from the seafloor to planetary surfaces.

INTRODUCTION

Single-thread channels abound on planetary surfaces with varied fluids and substrates (Komatsu and Baker, 1996; Karlstrom et al., 2013; Allen and Pavelsky, 2018; Fig. 1). All natural channels, including rivers, invariably deviate from straight-line paths, with typical sinuosity values (ratio of along-channel to straight-line distance) up to ~3 (Leopold and Wolman, 1957; Howard and Hemberger, 1991). Sinuosity is the most widely used statistic to describe river planform geometry and has been interpreted as a proxy for environmental processes including climate (Stark et al., 2010), the stabilizing effects of vegetation and fine sediment (Braudrick et al., 2009; Davies and Gibling, 2010; Lapôtre et al., 2019), tectonics, geologic structure, and lithology (Harden, 1990; Johnson and Finnegan, 2015).

However, to provide a window into past landscape conditions, sinuosity must respond to those conditions over time. Some rivers show abundant evidence for sinuosity evolution as recorded by direct observations or geologic markers like cutoffs (Fig. 1A), scroll bars, terraces, and eroded valley margins (Hooke, 2013). Yet many rivers lack these indicators of channel migration (Fig. 1B), suggesting that river sinuosity may, to some degree, form randomly at channel inception in response to intrinsic irregularities of topography (Mueller, 1968). Extreme examples of channelization also demonstrate extrinsic controls on sinuosity such as crevasses that steer supraglacial meanders (Fig. 1C) and sinuous volcanic channels that show little evidence of migration (Fig. 1D). Ambiguity in the origin of sinuosity calls into question its utility for interpreting environmental history. For example, a classic debate regarding bedrock-bound meanders centers on whether high sinuosity due to channel migration is a relic of previous alluvial states (Winslow, 1893). We consider a broader question: for any channel, under what conditions is sinuosity a diagnostic of channel migration? We propose that the magnitude of sinuosity can distinguish whether the channel form is consistent with randomness or has instead developed mainly through ordered growth by channel migration.

For single-thread rivers, theoretical models describe two end-member scenarios for the origin of sinuosity, which we define as random models and migration models, respectively. Random models treat the path of the centerline (the line equidistant between each of the river banks) as a random walk (Langbein and Leopold, 1966). In contrast, migration models explain sinuosity development by explicitly considering hydrodynamic effects that erode and construct river banks and grow meander bends (Camporeale et al., 2007). Neither class of models fully captures river forms. Geometric analyses show that compared to natural channels, centerlines made by pure random walks change direction too quickly and form tangled loops rather than alternating bends (Ferguson, 1976); channel-migration models generate bends, but they are overly regular and sinuous (Howard and Hemberger, 1991). Therefore, to better mimic the geometry of natural channels, a model requires spatial memory at relatively small length scales but irregularity at larger scales.

Many natural time series, such as climatological data, can likewise be described by a combination of inertia and randomness. A first-order autoregressive process (AR-1) is recognized as the simplest possible model—and the default expectation—for any geophysical process that is both dependent on previous states and subject to random disturbances (Roe, 2009). Ferguson (1976) showed that compared to an AR-1 model, a second-order autoregressive model (AR-2)

CITATION: Limaye, A.B., et al., 2021, River sinuosity describes a continuum between randomness and ordered growth: Geology, v. 49, p. , https://doi.org/10.1130/G49153.1

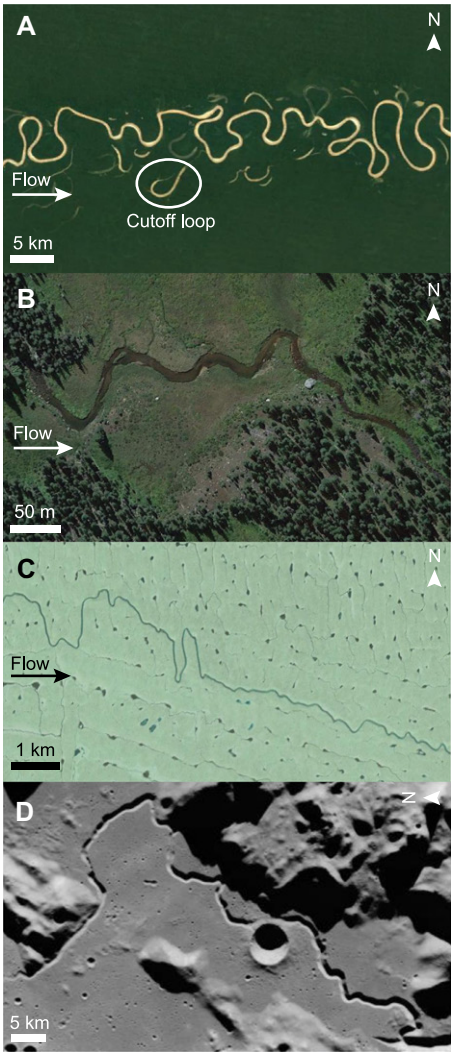

Figure 1. Natural, single-thread channels in varied environments. (A) The Juruá River, Peru (6.5°S, 69.0°W), an alluvial river with abundant geologic indicators of channel migration. (B) Fall Creek, Colorado, USA (39.5°N, 106.4°W), which has scant indicators of channel migration (Howard, 1996). (C) A sinuous channel on the Greenland ice sheet (79.5°N, 21.0°W) with relatively straight segments that align with crevasses (Chu, 2014). (D) Hadley Rille, a channel on the Moon (27.0°N, 3.0°E; NASA/GSFC/ASU), is interpreted as a collapsed lava tube (Howard et al., 1972). Images in A–C: Landsat/USGS/Google Earth™.

tempers high-frequency variations while still allowing overall bend shapes to vary. That means the AR-2 model represents the simplest model for sinuosity that yields shapes comparable to natural channels. The AR-2 model is strictly geometric and is therefore sufficiently generic to describe channels whose formation processes may differ in detail. For natural channels that lack indicators of channel migration, we propose that spatially correlated randomness as expressed by the AR-2 model represents the null hypothesis for river sinuosity and can be used to test the significance of environmental interpretations.

MODELING AND ANALYSIS OF CHANNEL PLANFORMS

We systematically characterized the AR-2 model and quantitatively compared its outputs to natural channels to predict the natural range of river sinuosity due to initial randomness in the channel path. To interpret the evolution of sinuosity from its random initial condition, we evolved select AR-2 model outputs using a simple, curvature-driven model for channel migration (see the Supplemental Material[1]). The AR-2 model, a discrete approximation of a differential equation (Ferguson, 1976), is

$$\theta_i = b_1\theta_{i-1} + b_2\theta_{i-2} + \epsilon_i, \quad (1)$$

where θ is the azimuth of the channel centerline, i is the index of the centerline node, b_1 and b_2 are coefficients, and ϵ is a random series of direction disturbances drawn independently from a normal distribution with a mean of zero and variance of σ^2.

For a global data set of natural channels, we calculated sinuosity and fit AR-2 model parameters to constrain their ranges (Fig. S1 in the Supplemental Material). We then used a suite of model runs to estimate the magnitude of sinuosity (S) that can be explained with Equation 1 using a systematic parameter sweep for b_1, b_2, and σ. For each parameter combination, we analyzed 100 replicates with different disturbance series (ϵ) to statistically characterize model randomness (Figs. S2 and S3). Because in some model runs the channel crossed itself, we treated each self-intersection as a cutoff loop and removed it to maintain a simplified, continuous centerline. For each set of replicates, we calculated the mean and standard deviation of sinuosity of the simplified centerlines and the average length of the original centerlines bound in self-intersecting loops.

RESULTS

The suite of model runs shows that both sinuosity and the degree of self-intersection vary systematically with b_1, b_2, and σ (Fig. 2A). Higher values of b_1 and σ increase sinuosity, with mean values typically <1.5. The inherent randomness in the model causes sinuosity to vary across the replicate simulations (Fig. 2B). For a fraction of the replicates, S is >1.5, particularly where self-intersection is common or $\sigma \geq 0.3$ (Fig. 2C); the latter rarely occurs in nature (Fig. S1). These model results imply that randomly generated sinuosity rarely exceeds 1.5 for channels that are both geometrically realistic and have not migrated. We hypothesize that a channel typically only reaches $S > 1.5$ by migrating.

To explore this hypothesis, we consider a scenario wherein an initial centerline created via the random model evolves through channel migration driven by centerline curvature (see the Supplemental Material). A dimensionless form of time (t^*) is used to track the cumulative channel migration,

$$t^* = \frac{tE_L}{w_c}, \quad (2)$$

where t is dimensioned time, E_L is maximum lateral erosion rate, and w_c is channel width. In this scenario, the channel begins with a low sinuosity caused by randomness ($S = 1.1$ at $t^* = 0$; Fig. 3A). Subsequent channel migration causes increased sinuosity by elongating half-meanders between curvature inflections (Fig. 3B; Howard and Hemberger, 1991). Importantly, AR-2 randomness cannot generate half-meanders of comparable length because the sense of curvature reverses over shorter distances along-stream. This behavior ultimately limits the range of sinuosity that randomness can generate absent extrinsic factors.

The migration model further shows that bends in initially random channels with different sinuosity follow offset trajectories for sinuosity growth through channel migration (Fig. 3C). These cases arrive, at different dimensionless times, at a critical sinuosity that suggests channel migration ($S_c = 1.5$). As expected, the dimensionless time to reach the critical sinuosity (t_c^*) generally decreases with increasing initial sinuosity (Fig. 3D). Moreover, t_c^* is <15 in all cases, which suggests an upper bound on the amount of channel migration that must occur before the centerline conclusively reflects channel migration. In other words, the initial, random sinuosity of the channel is overwritten over a finite time interval.

For a global data set of river planforms, sinuosity mostly varies from 1 to 2.5 (Fig. 4A). We fit the AR-2 model to each observed planform to find the corresponding distribution of sinuosity values predicted by the model. For model cases with no self-intersection in the original centerline, the probability of the random sinuosity exceeding the observed sinuosity (S_{obs}) is significant for $S_{obs} < 1.2$ but declines sharply with increasing S_{obs} (Fig. 4B). If cases with self-intersection in the original centerline are considered, the random model accounts for a greater range of S_{obs} but is unlikely to account for $S_{obs} > 2$ (Fig. 4C). A separate data set of channels with documented migration (Fig. 4D) shows that migration favors higher sinuosity values, including $S > 1.5$ for all cases in the Andean foreland with especially high migration rates ($>10\%$ w_c per year; Sylvester et al., 2019). Substituting $t_c^* = 15$ and these observed migration rates in

[1]Supplemental Material. Additional methods. Please visit https://doi.org/10.1130/GEOL.S.15152385 to access the supplemental material, and contact editing@geosociety.org with any questions.

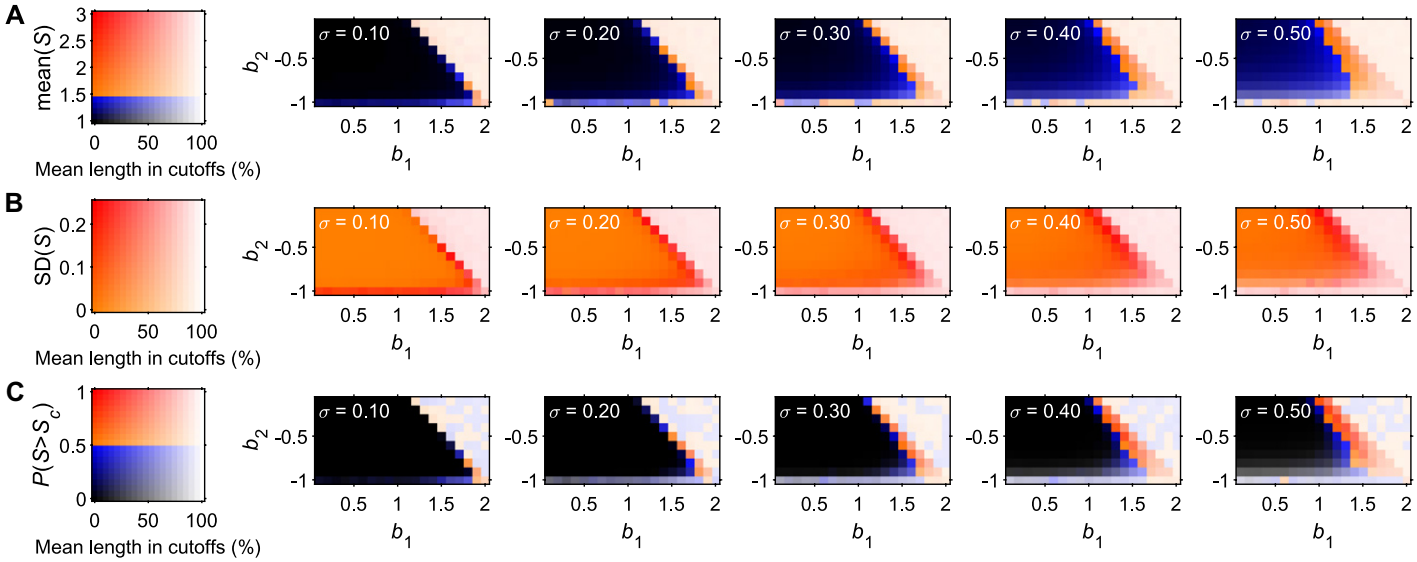

Figure 2. Effects of AR-2 model parameters (Equation 1) on sinuosity (*S*). Each panel shows a phase space in the parameters b_1 and b_2 for a fixed value of σ; each pixel represents 100 replicate model runs from different random disturbance series (ϵ). Transparency in each color scale represents the average fraction of the original centerline composed by cutoff loops. (A) Mean sinuosity. (B) Standard deviation of sinuosity. (C) The exceedance probability for a critical sinuosity (S_c = 1.5).

Equation 2, for the Andean foreland rivers we estimate that the time scale to critical sinuosity ($S_c = 1.5$)—the clear distinction from randomness in the planform—is $t_c \approx 150$ years.

DISCUSSION AND CONCLUSIONS

We used a null-hypothesis test to estimate the role of spatially correlated randomness in river channel sinuosity (*S*) and show that a random model typically produces $S < 1.5$ (Fig. 2A). The low probability of exceeding this critical value ($S_c = 1.5$; Fig. 2C) indicates that for channels with $S > S_c$, the null hypothesis can be rejected, and that non-random, ordered channel migration is a necessary condition for the sinuosity observed. The converse ($S < S_c$)—not rejecting the null hypothesis—does not imply that randomness fully explains the observed sinuosity. Migrating channels with $S < S_c$ are relatively common (Fig. 4D); relatively low sinuosity in migrating channels could result from slow channel migration and/or limited evolution time (Equation 2) or extrinsic constraints. Thus, although the sinuosity criterion cannot rule out migration if $S < S_c$, the metric does identify cases in which channel migration is definitive ($S > S_c$).

A quantitative signature of migration in river sinuosity lends this common characteristic further significance for interpreting landscape history. Sinuosity in natural channels reflects neither pure randomness nor universal channel migration but rather exists on a continuum between the two. To borrow from Shakespeare's *Twelfth Night*, some channels are born sinuous (Fig. 1D); some achieve further sinuosity, through channel migration (Fig. 1A); and some have sinuosity thrust upon them, by faulting, valley shape, or other non-random topographic control (Fig. 1C). Random, initial sinuosity is embellished to a degree determined by the rate and duration of channel migration (Fig. 3C). Spatial correlation should be considered for initial planform geometry in numerical models of channel migration, as this geometry and its persistence through time (Fig. 3D) are more realistic than the uncorrelated, ephemeral noise that is most often used (e.g., Frascati and Lanzoni, 2010). At quasi-steady-state, such channel-migration models can develop sinuosity ($S > 3.5$) that exceeds typical observations (Fig. 4A; Howard, 1996; Frascati and Lanzoni, 2010). Therefore, in the absence of evidence indicating channel migration, spatially correlated randomness should represent the null hypothesis for sinuosity.

In rivers characterized by channel migration and non-local avulsions, a given channel may express the two regimes of the randomness-order continuum both in space and over time (Valenza et al., 2020). When a river avulses to create a diversion across its own floodplain, it may reoccupy relict channels and/or cut new ones. An avulsing channel may therefore simultaneously form new reaches guided by random landscape disturbances and also inherit the bends of an antecedent, migrating channel. As the planform of the avulsion channel evolves with bend migration, indicators of its randomness are overwritten.

Our findings can inform interpretations of environmental forcing from the sinuosity of natural channels. For example, Stark et al. (2010) interpreted climate forcing from a spatial trend in sinuosity for mixed bedrock-alluvial rivers with reported sinuosity $S < 1.5$, which is the critical value that we identify. Our analysis suggests that using sinuosity as a proxy for the degree of channel migration should be done with caution for rivers with sinuosity below the critical value; future analyses could account for the role of random sinuosity as a null hypothesis. Our results suggest that river sinuosity could, however, be used to infer alluvial sediment deposited by channel migration in a channel belt many times wider than the river itself (Jobe et al., 2016). This approach could inform predictions for stratigraphic architecture in cases where channel belts are not directly observable as in some seismic images of marine sediments (Pirmez and Imran, 2003) and on planetary surfaces (Burr et al., 2013). Finally, these results may apply to optimizing river restoration projects, which are commonly designed to match idealized meandering forms (Kondolf, 2006). Our analysis shows that for cases where migration by the original channel exhibited minimal migration, restored channels should have low sinuosity ($S < 1.5$). Meanwhile, natural, rapidly migrating channels drive forest disturbance and primary succession that may contribute to biodiversity (Salo et al., 1986). These observations suggest that high-sinuosity ($S > 2$) river corridors, which are likely dominated by migration and relatively rare (Figs. 4A and 4D), should be prioritized for conservation.

ACKNOWLEDGMENTS

We thank Samuel Johnstone and an anonymous reviewer for helpful comments, and Roman DiBiase, Douglas Edmonds, and Chris Paola for discussions. The U.S. National Science Foundation (grants EAR-1823530 and EAR-1246761), the British Society for Geomorphology, and Los Alamos National Laboratory (LDRD-20170668PRD1) supported this work. Data and code from this study are available at the University of Virginia's (USA) data repository LibraData (https://doi.org/10.18130/V3/TRTTIS) and at Github (https://github.com/alimaye/AR2-sinuosity), respectively.

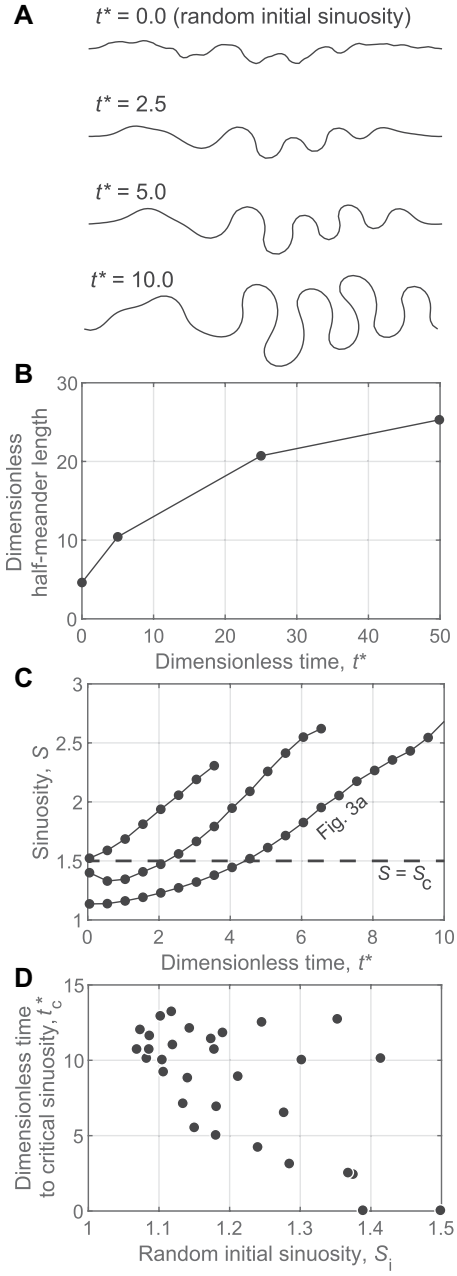

Figure 3. Sinuosity evolution by channel migration. (A) A centerline with randomly generated sinuosity (AR-2 model) is evolved with the channel migration model. (B) Length of half-meander bends (84th percentile) versus dimensionless time, *t (Equation 2). (C) Sinuosity versus *t** for three different values of random initial sinuosity. (D) Elapsed *t** for development of critical sinuosity (S_c = 1.5) versus random initial sinuosity.**

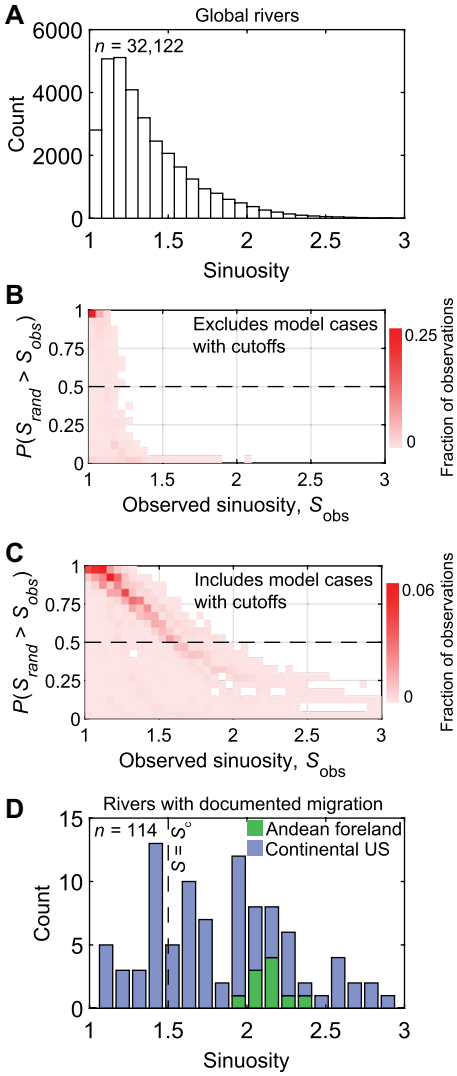

Figure 4. Sinuosity of natural channels. (A) Histogram of sinuosity for globally distributed, natural channels (Allen and Pavelsky, 2018) and corresponding exceedance probability in the AR-2 model excluding (B) and including (C) self-intersecting cases. In B and C, S_{rand} and S_{obs} indicate modeled and observed sinuosity, respectively, and the dashed lines indicate 50% exceedance probability. (D) Histogram of sinuosity for natural channels with documented channel migration in the Andean foreland (Sylvester et al., 2019; green) and the continental United States (Lagasse et al., 2004; blue).

REFERENCES CITED

Allen, G.H., and Pavelsky, T.M., 2018, Global extent of rivers and streams: Science, v. 361, p. 585–588, https://doi.org/10.1126/science.aat0636.

Braudrick, C.A., Dietrich, W.E., Leverich, G.T., and Sklar, L.S., 2009, Experimental evidence for the conditions necessary to sustain meandering in coarse-bedded rivers: Proceedings of the National Academy of Sciences of the United States of America, v. 106, p. 16,936–16,941, https://doi.org/10.1073/pnas.0909417106.

Burr, D.M., Perron, J.T., Lamb, M.P., Irwin, R.P., Collins, G.C., Howard, A.D., Sklar, L.S., Moore, J.M., Ádámkovics, M., and Baker, V.R., 2013, Fluvial features on Titan: Insights from morphology and modeling: Geological Society of America Bulletin, v. 125, p. 299–321, https://doi.org/10.1130/B30612.1.

Camporeale, C., Perona, P., Porporato, A., and Ridolfi, L., 2007, Hierarchy of models for meandering rivers and related morphodynamic processes: Reviews of Geophysics, v. 45, https://doi.org/10.1029/2005RG000185.

Chu, V.W., 2014, Greenland ice sheet hydrology: A review: Progress in Physical Geography, v. 38, p. 19–54, https://doi.org/10.1177/0309133313507075.

Davies, N.S., and Gibling, M.R., 2010, Cambrian to Devonian evolution of alluvial systems: The sedimentological impact of the earliest land plants: Earth-Science Reviews, v. 98, p. 171–200, https://doi.org/10.1016/j.earscirev.2009.11.002.

Ferguson, R.I., 1976, Disturbed periodic model for river meanders: Earth Surface Processes, v. 1, p. 337–347, https://doi.org/10.1002/esp.3290010403.

Frascati, A., and Lanzoni, S., 2010, Long-term river meandering as a part of chaotic dynamics? A contribution from mathematical modelling: Earth Surface Processes and Landforms, v. 35, p. 791–802, https://doi.org/10.1002/esp.1974.

Harden, D., 1990, Controlling factors in the distribution and development of incised meanders in the central Colorado Plateau: Geological Society of America Bulletin, v. 102, p. 233–242, https://doi.org/10.1130/0016-7606(1990)102<0233:CFITDA>2.3.CO;2.

Hooke, J.M., 2013, 9.16 River meandering: Treatise on Geomorphology, v. 9, p. 260–288, https://doi.org/10.1016/B978-0-12-374739-6.00241-4.

Howard, A.D., 1996, Modelling channel evolution and floodplain morphology, *in* Anderson, M.G., Walling, D.E., and Bates, P.E. eds., Floodplain Processes: Chichester, UK, John Wiley and Sons, Ltd., p. 15–62.

Howard, A.D., and Hemberger, A.T., 1991, Multivariate characterization of meandering: Geomorphology, v. 4, p. 161–186, https://doi.org/10.1016/0169-555X(91)90002-R.

Howard, K.A., Head, J.W., and Swann, G.A., 1972, Geology of Hadley Rille: Geochimica et Cosmochimica Acta, v. 1, p. 1–14.

Jobe, Z.R., Howes, N.C., and Auchter, N.C., 2016, Comparing submarine and fluvial channel kinematics: Implications for stratigraphic architecture: Geology, v. 44, p. 931–934, https://doi.org/10.1130/G38158.1.

Johnson, K.N., and Finnegan, N.J., 2015, A lithologic control on active meandering in bedrock channels: Geological Society of America Bulletin, v. 127, p. 1766–1776, https://doi.org/10.1130/B31184.1.

Karlstrom, L., Gajjar, P., and Manga, M., 2013, Meander formation in supraglacial streams: Journal of Geophysical Research: Earth Surface, v. 118, p. 1897–1907, https://doi.org/10.1002/jgrf.20135.

Komatsu, G., and Baker, V.R., 1996, Channels in the solar system: Planetary and Space Science, v. 44, p. 801–815, https://doi.org/10.1016/0032-0633(96)00010-4.

Kondolf, G.M., 2006, River restoration and meanders: Ecology and Society, v. 11, p. 42, https://doi.org/10.5751/ES-01795-110242.

Lagasse, P.F., Zevenbergen, L.W., Spitz, W.J., and Thorne, C.R., 2004, Methodology for predicting channel migration: Transportation Research Board of the National Academies, https://doi.org/10.17226/23352.

Langbein, W.B., and Leopold, L.B., 1966, River meanders: Theory of minimum Variance: U.S. Geological Survey Professional Paper 422-H, 16 p., https://doi.org/10.3133/pp422H.

Lapôtre, M.G.A., Ielpi, A., Lamb, M.P., Williams, R.M.E., and Knoll, A.H., 2019, Model for the formation of single-thread rivers in barren landscapes and implications for pre-Silurian and Martian fluvial deposits: Journal of Geophysical Research: Earth Surface, v. 124, p. 2757–2777, https://doi.org/10.1029/2019JF005156.

Leopold, L.B., and Wolman, M.G., 1957, River channel patterns: Braided, meandering, and straight: U.S. Geological Survey Professional Paper 282-B, p. 39–85, https://doi.org/10.3133/pp282B.

Mueller, J.E., 1968, An introduction to the hydraulic and topographic sinuosity indexes: Annals of the Association of American Geographers, v. 58, p. 371–385, https://doi.org/10.1111/j.1467-8306.1968.tb00650.x.

Pirmez, C., and Imran, J., 2003, Reconstruction of turbidity currents in Amazon Channel: Marine and Petroleum Geology, v. 20, p. 823–849, https://doi.org/10.1016/j.marpetgeo.2003.03.005.

Roe, G., 2009, Feedbacks, timescales, and seeing red: Annual Review of Earth and Planetary Sciences, v. 37, p. 93–115, https://doi.org/10.1146/annurev.earth.061008.134734.

Salo, J., Kalliola, R., Häkkinen, I., Mäkinen, Y., Niemelä, P., Puhakka, M., and Coley, P.D., 1986, River dynamics and the diversity of Amazon lowland forest: Nature, v. 322, p. 254–258, https://doi.org/10.1038/322254a0.

Stark, C.P., Barbour, J.R., Hayakawa, Y.S., Hattanji, T., Hovius, N., Chen, H., Lin, C.-W., Horng, M.-J., Xu, K.-Q., and Fukahata, Y., 2010, The climatic signature of incised river meanders: Science, v. 327, p. 1497–1501, https://doi.org/10.1126/science.1184406.

Sylvester, Z., Durkin, P., and Covault, J.A., 2019, High curvatures drive river meandering: Geology, v. 47, p. 263–266, https://doi.org/10.1130/G45608.1.

Valenza, J.M., Edmonds, D.A., Hwang, T., and Roy, S., 2020, Downstream changes in river avulsion style are related to channel morphology: Nature Communications, v. 11, p. 2116, https://doi.org/10.1038/s41467-020-15859-9.

Winslow, A., 1893, The Osage River and its meanders: Science, v. 22, p. 31–32, https://doi.org/10.1126/science.ns-22.546.31.

Printed in USA